

RESEARCH ARTICLE

Energy-Efficient CoMP Joint Transmission in Hybrid-Powered mmWave Networks

SEUNG-YEON KIM¹ AND HANEUL KO², (Member, IEEE)¹Department of Computer Convergence Software, Korea University, Sejong 30019, South Korea²Department of Electronic Engineering, Kyung Hee University, Yongin, Gyeonggi 17104, South Korea

Corresponding author: Haneul Ko (heko@khu.ac.kr)

This work was supported by the Basic Science Research Program through the National Research Foundation of Korea (NRF) funded by the Ministry of Education under Grant NRF-2021R111A3042204.

ABSTRACT In the downlink of millimeter wave (mmWave) cellular networks, coordinated multi-point transmission (CoMP) with the joint transmission (JT) strategy can achieve a higher data rate at cell edge by multiple desired signals. However, since cooperative transmissions among multiple cells lead to increased energy consumption for these cells, an energy efficient CoMP-JT strategy is required. In this paper, we propose an energy efficient CoMP-JT (EE-CoMP) scheme with hybrid power, where a small cell base station (SC) can use both renewable power and grid power. In EE-CoMP, when the multiple neighboring SCs conduct a cooperative transmission, these SCs determine whether or not to conduct CoMP-JT in a distributed manner. To minimize the grid energy consumption of SCs while maintaining the outage probability, we consider a stochastic game model with constraints for an EE-CoMP based system. In this way, the policy for conducting CoMP-JT can be obtained by applying a best response algorithm. Evaluation results show that EE-CoMP can reduce the grid energy consumption by 80% compared with a probability-based scheme while providing a sufficiently target outage probability (e.g., 0.1).

INDEX TERMS Millimeter wave, coordinated multi-point transmission, 5G, hybrid-power, energy efficiency.

I. INTRODUCTION


In the fifth generation (5G) of cellular networks, millimeter wave (mmWave) is considered a promising technology that can meet the user demand for significantly improved performance with higher data rates [1]. Then, those demands can be achieved by a spectrum expansion for largely unused spectrum [2]. Moreover, for high traffic volumes of users in mmWave-enabled Internet of Things (IoT) networks, more small cells (SCs) are deployed to improve the capacities [3]. However, in mmWave cellular networks with dense SCs, the users around an edge of a SC still suffer from intercell interferences (ICIs) [4]. Further, the data rates can be significantly decreased by the blockage effect [5]. To overcome these problems for mmWave SC, as a cooperation diversity technique, a coordinated multipoint transmission and

reception (CoMP) has been considered [6], [7]. In particular, CoMP with a joint transmission (CoMP-JT) scheme can achieve an increased signal-to-interference and noise ratio (SINR), where the user can coherently receive the desired signal from not only its serving cell but also an adjacent cell [8].

Although CoMP-JT in dense mmWave networks can provide higher data rates to the users, it has some drawbacks for a system, such as the additional energy consumption caused by a cooperative transmission of SC [9]. Therefore, to reduce the energy consumption, in this paper, we propose an energy-efficient CoMP-JT scheme (EE-CoMP) in which each SC can use hybrid power, such as both a grid and a renewable energy source [10].

II. RELATED WORK AND MAIN CONTRIBUTIONS

A number of studies have attempted to improve the energy efficiency of SC and the data rate of users in mmWave cellular

The associate editor coordinating the review of this manuscript and approving it for publication was Masood Ur-Rehman .

networks [11], [12], [13], [14], [15], [16], [17], [18], [19], [20], [21], [22]. For example, [11], [12], [13], [14], [15], and [16] introduced the dual-powered system for the energy efficiency in cellular network. In [11], the authors showed that dual-powered system can provide a seamless operation of the base stations (BSs) without energy outages. Balakrishnan et al. [12] showed the impact of dual-powered BS for traffic-energy imbalance. Al Haj Hassan et al. [13] considered stochastic environments such as harvested energy and channel conditions for dual-powered networks. The results from [12] and [13] demonstrated that the dual powered system can increase the revenue gain while guaranteeing user requirements such as delay constrained and tolerance. In [14], the authors proposed an energy sharing based cooperative framework for dual-powered BS wherein a BS that is not experiencing an energy outage can conduct the energy cooperation. Li et al. [15] designed a energy efficient mmWave cellular networks where SCs harvest electromagnetic energy and optimized the transmission power of SCs by formulating a fractional programming problem and exploiting several mathematical methods (i.e., Dinkerbach and Lagrange dual decoupling). Liu et al. [16] proposed a cost-aware online resource management algorithm for energy cost minimization for cellular networks with renewable and grid energy power. The results showed that the proposed algorithm could determine the optimal solution between the energy cost and the queue backlog.

To increase the data rate of users in mmWave cellular networks, [17], [18], [19], [20], [21], [22] considered cooperative transmission technology. In [17], the authors showed the impact of a dual link by cooperative transmission for blocking objects such as stochastic geometry and random shape. Gerasimenko et al. [18] established the user performance model for the connectivity strategy in dense mmWave SC, which is determined according to SC density and height as well as blocker density. The results showed that the multi-connectivity mechanism in mmWave SCs can improve the capacity of the user. In [19], the authors proposed a dynamic control algorithm to improve the power-efficient, highly reliable, and low-latency, where the CoMP serving set from SCs is selected dynamically by exploiting the queue and channel states. Zhao et al. [20] introduced the three CoMP strategies to improve the coverage probability and the mean local delay in the mmWave cellular networks, where the three strategies are fixed-number BS cooperation (FRC), fixed-region BS cooperation (FNC), and interference-aware BS cooperation (IAC). The results showed that the performance of the IAC outperforms other schemes for the high density of BSs. Arfaoui et al. [21] introduced two multiple access schemes using zero-forcing pre-coding technique to increase the data rate of users. In [22], the authors proposed a CoMP enabled heterogeneous network with a hybrid-powered to maximize the system energy efficiency, where hybrid power is allocated by considering the energy consumption.

However, no previous work has optimized the energy efficiency and outage probability for mmWave networks using

CoMP-JT in a distributed manner.¹ In our proposed scheme, when the users require increased data rates, the additional assistance of multiple SCs (using CoMP-JT) is conducted, where each SC can use hybrid power such as grid and renewable power. However, the excessively blackundant cooperative transmissions of the SCs can lead to diminished energy efficiency. Therefore, in our scheme, the cooperative SCs determine whether or not to conduct CoMP-JT in a distributed manner, where the grid energy consumption and the outage probability of SCs are considered. To optimize the trade-off between the grid energy consumption and the outage probability, we formulate a constrained stochastic game model. The solution of the game model is obtained using a best response algorithm. The results show that EE-CoMP can decrease the grid energy consumption compared to that of a probability-based scheme while providing a sufficient target outage probability.

The contributions of our paper can be summarized as follows: 1) The energy efficient mmWave network system using CoMP-JT is proposed in which cooperative SCs selectively conduct CoMP-JT; 2) Unlike the conventional centralized approaches, for an EE-CoMP-based system, we obtain the optimal policy regarding the behavior of cooperative SCs in a distributed manner, where a stochastic game model with constrains is formulated; and 3) We evaluate EE-CoMP under various environments, which are used to provide guidelines for the design of EE-CoMP-based mmWave systems.

The rest of this paper is organized as follows. Section III describes the EE-CoMP-based mmWave system. In Section IV, the constrained stochastic game model is formulated. Section V presents the numerical examples, and Section VI provides concluding remarks.

III. SYSTEM MODEL

Fig. 1 shows the two scenarios of an EE-CoMP-based mmWave network system wherein, since each SC has energy harvesting capability, renewable power and grid power can both be used. Moreover, we consider the downlink of mmWave cellular networks where SCs use CoMP-JT to achieve a higher data rate. That is, the user can receive the desired signals from multiple SCs. In scenario (a), SC 1 and SC 2 conduct the CoMP-JT while, since SC 3 does not have renewable energy, it does not conduct the CoMP-JT. Further, although SC 4 does not have renewable energy, it conducts CoMP-JT to provide higher data rate for the user. Thus, the grid energy of SC 4 is used. For a scenario (b), the user can receive the desired signals from SC 1 and SC 2 with renewable energy. On the other side, although SC 4 has renewable energy, it does not conduct the CoMP-JT to the user, where the desired signal power level for the user only satisfies two

¹To optimize the energy efficiency and outage probability for mmWave networks, we can introduce a centralized approach where a central server (e.g., central cloud) can collect all state information and derive the optimal stationary policy of all SCs. However, this approach may lead to high signaling overhead and a single point of bottleneck/failure. Therefore, we introduce a distributed approach.

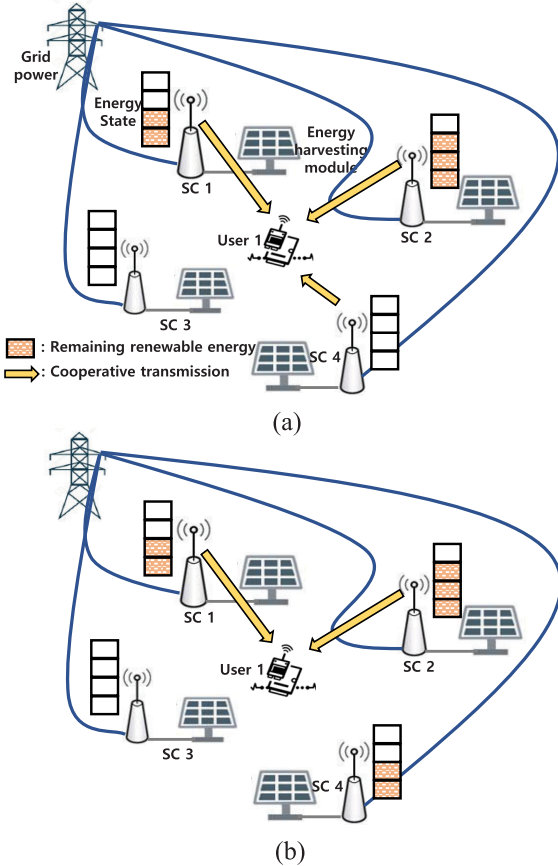


FIGURE 1. Two scenarios of EE-CoMP-based mmWave network system.

signals. Thus, in this case, the grid and renewable energies can both be saved.

As shown in these scenarios, several SCs can conduct CoMP-JT to the user (e.g., SC 1, SC 2, and SC 4 in scenario (a)). However, in scenario (a), if it is assumed that the user has a sufficient SINR even without CoMP-JT of SC 4, CoMP-JT of SC 4 can be considered as unnecessary transmission. Moreover, in this scenario, since SC 4 conducts CoMP-JT by using the grid energy, lower energy efficiency is inevitably achieved. To mitigate this problem, in our proposed system, each SC decides whether or not to conduct CoMP-JT by considering the actions of other SCs. In so doing, as in scenario (b), if the user can have a sufficient SINR from the CoMP-JT of SC 1 and SC 2, SC 4 does not conduct the CoMP-JT to the user although SC 4 has renewable energy. Then, this saved renewable energy can be used for subsequent transmission. Note that, for the optimal decision on whether or not to conduct CoMP-JT by considering the actions of other SCs, we introduce the stochastic game model, which will be elaborated in Section IV.

In our system model, we consider the outdoor dense mmWave networks. For a propagation model, the signal power received at a user from SC i , i.e., P_i , is expressed as

$$P_i = P_t r_i^{-\alpha} h_i, \quad (1)$$

TABLE 1. Summary of notations.

Notation	Description
S_i	Local state space of SC i
S_{-i}	State space of all SCs except SC i
S	Global state space
E_{max}	Total renewable energy capacity of SC
E_i	Renewable energy level of SC i
A_i	Local action set of SC i
A	Global action space
N_i	Number of users in SC i
$P_E(\lambda_E, k)$	Probability that a SC has the harvested energy k for a mean λ_E .
$P_U(\lambda_U, k)$	Probability that the number of arrived users is k for a mean λ_U .
σ^2	Noise power
ψ_G	Average grid energy consumption
ψ_o	Average outage probability
γ_o	Target outage probability
P_t	Transmission power of SC

where P_t is the transmit power of SC, and $r_i^{-\alpha}$ denotes a path-loss at a distance r_i between SC i and a user, where α denotes the path-loss exponent. Further, h_i indicates the small-scale fading, which is a normalized Gamma random variable with parameter m , i.e., $h_i \sim \Gamma(m, 1/m)$. Note that mmWave links are generally well-modeled by Nakagami fading [23].

For a conventional cellular network system, according to Eq. (1), the SINR of the average power received at a user is as follows:

$$\text{SINR} = \frac{P_0}{\sum I + \sigma^2}, \quad (2)$$

where P_0 is the received signal power from a target SC, $\sum I$ and σ^2 respectively denote the sum of interference power and additive noise.

IV. STOCHASTIC GAME MODEL AND OPTIMIZATION FORMULATION

In a stochastic game model with constraints, SCs and players are used interchangeably. Therefore, in our formulation, SC i and player i have the same meaning.

A. LOCAL STATE SPACE

Each SC i has a finite local state space S_i . The local state space, S_i , can be defined as

$$S_i = E_i \times N_i, \quad (3)$$

where E_i and N_i denote the renewable energy levels of SC i and the state space for the number of users in SC i , respectively. E_i can be defined as

$$E_i = \{0, 1, \dots, E_{max}\}, \quad (4)$$

where E_{max} denotes the renewable energy capacity of SC i . N_i can be represented by

$$N_i = \{0, 1, \dots, N_{max}\}, \quad (5)$$

where N_{max} denotes the maximum number of users in SC coverage. Note that N_{max} depends on the capacity of SC i . In addition, $S = \prod_i S_i$ denotes a global state space, where \prod is the Cartesian product. Then, $S_{-i} = \prod_{j \neq i} S_j$ is the state space of all SCs except SC i .

B. ACTION SPACE

Since SC i can decide whether to conduct CoMP-JT or not, a finite local action set of SC i , A_i , can be represented by

$$A_i = \{0, 1\}, \tag{6}$$

where $A_i = 0$ means that SC i does not conduct CoMP-JT, whereas $A_i = 1$ indicates that SC i conducts CoMP-JT. A global action space A can be denoted by $A = \prod_i A_i$.

C. TRANSITION PROBABILITY

In our proposed system, when there are the users in the coverage of SC i and SC i conducts CoMP-JT, its renewable energy level E_i decreases. Therefore, E_i is affected by N_i and A_i . Meanwhile, E_i and N_i change independently with each other. To summarize, for the chosen action A_i , the transition probability from the current state, $S_i = [E_i, N_i]$, to the next state, $S_{i'} = [E_{i'}, N_{i'}]$ can be described by

$$P[S_{i'}|S_i, A_i] = P[E_{i'}|E_i, N_i, A_i] \times P[N_{i'}|N_i]. \tag{7}$$

In Eq. (7), for $P[E_{i'}|E_i, N_i, A_i]$, we assume that the harvested energy k during the decision epoch at SC i follows the Poisson distribution with mean λ_E , $P_E(\lambda_E, k)$ for the tactical modeling as in [29].² That is, we assume that when SC i does not conduct CoMP-JT (i.e., $A_i = 0$), the renewable energy level of SC i in the next state, $E_{i'}$, increases by k with the probability $P_E(\lambda_E, k)$, where SC i cannot store renewable energy exceeding its capacity (i.e., $E_i \leq E_{max}$). Therefore, the corresponding probabilities can be defined as Eq. (8), shown at the bottom of the next page.

Meanwhile, for N_i number of users, when SC i conducts CoMP-JT (i.e., $A_i = 1$), E_i decreases by N_i , where if there is no sufficient renewable energy in SC i (i.e., $E_i < N_i$), then the grid energy in SC i is used as often as the insufficient renewable energy and $E_i = 0$. Therefore, the corresponding probabilities can be defined as Eq. (9), shown at the bottom of the next page.

Moreover, when we assume that the arrived users k during decision epoch in SC i follows the Poisson distribution with mean λ_U , $P_\lambda(\lambda_U, k)$, $P[N_{i'}|N_i]$ is defined by

$$P[N_{i'}|N_i] = \begin{cases} P_\lambda(\lambda_U, k), & \text{if } N_{i'} = k \\ 0, & \text{otherwise,} \end{cases} \tag{12}$$

where $N_i \leq N_{max}$.

D. COST FUNCTION

To minimize the grid energy consumption of SC i , we define the cost function $v(S_i, A_i)$, where when SC i conducts CoMP-JT (i.e., $A_i = 1$) and does not have sufficient renewable energy to service for users, n_i , (i.e., $E_i - n_i < 0$), the grid energy is used. That is, this case occurs when $E_i < n_i$. Therefore, the average used grid energy of this case can be

²Since the state in a stochastic game model is constructed in a discrete space, the continuous distribution like Gaussian distribution cannot be exploited for the transition probability. In addition, even though we have conducted extensive evaluations with other discrete distribution (e.g., Binomial and Geometric distribution, the similar trends on the numerical results can be obtained.

calculated as Eq. (10), shown at the bottom of the next page, where $|x|$ denotes the absolute value of x .

E. CONSTRAINT FUNCTION

To maintain the average outage probability, we define the constraint function $c(S_i, A_i)$, where it is defined that the outage occurs when the SINR is under threshold γ_{th} . For n neighbor SCs which can conduct CoMP-JT, the outage probability can be represented as Eq. (11), shown at the bottom of the next page, where λ^{-i} denotes the probability that at least one SC except for SC i conducts CoMP-JT. Further, $\mathcal{B}(j, \lambda^{-i}) = P_j r_j^{-\alpha} h_j \delta_j$, where δ_j denotes a delta function to return 1 if SC j conducts CoMP-JT with λ^{-i} . Otherwise, the function returns 0.

F. OPTIMIZATION FORMULATION

The stationary multi-policy of all SC, π , is to be optimized such that the long-term average grid energy consumption and the long-term average of outage probability constraint are both met. For this purpose, the long-term average grid energy consumption, $\psi_G(\pi)$, and the long-term average of outage probability, $\psi_o(\pi)$, are defined as

$$\psi_G(\pi) = \lim_{T \rightarrow \infty} \frac{1}{T} \sum_{t=1}^T E_\pi[v(S_t, A_t)] \tag{13}$$

and

$$\psi_o(\pi) = \lim_{T \rightarrow \infty} \frac{1}{T} \sum_{t=1}^T E_\pi[c(S_t, A_t)], \tag{14}$$

respectively, where $S_t \in S$ and $A_t \in 0, 1$ are the global state and action at time t , respectively. From Eqs. (13) and (14), the constrained stochastic game is formulated as follows:

$$\text{Minimize : } \psi_G(\pi) \tag{15}$$

$$\text{Subject to : } \psi_o(\pi) \leq \gamma_o, \tag{16}$$

where γ_o is the target average outage probability. The constrained Nash equilibrium is the solution of the formulated constrained stochastic game. Let π^* be the best response policy, which is the constrained Nash equilibrium when the following condition is satisfied.

$$\psi_G(\pi^*) \leq \psi_G((\pi^i, \pi^{-i})), \tag{17}$$

where π^i and π^{-i} respectively denote a stationary policy of SC i and a stationary policy of all SCs except SC i , and $\pi^* = (\pi^i, \pi^{-i})$. To obtain π^* , we apply a linear programming (LP) approach. Let $\phi^{i, \pi^{-i}}(S_i, A_i)$ be the stationary probability in local state S_i and action A_i of the SC i given the policies of the other SCs π^{-i} . Then, the equivalent LP model can be formulated and its solution $\phi^{i, \pi^{-i}}(S_i, A_i)$ can be interpreted as the optimal policy of the formulated game [24], [25]. The LP problem corresponding to Eqs. (15) and (16) can therefore be expressed as follows:

$$\text{Minimize : } \psi_G(\pi) = \sum_S \sum_A \phi^{i, \pi^{-i}}(S_i, A_i) v(S_i, A_i) \tag{18}$$

$$\text{s.t. } \sum_S \sum_A \phi^{i, \pi^{-i}}(S_i, A_i) c(S_i, A_i) \leq \gamma_o \tag{19}$$

$$\sum_A \varphi^{i,\pi^{-i}}(S_{i'}, A_i) = \sum_S \sum_A \varphi^{i,\pi^{-i}}(S_i, A_i) P[S_{i'}|S_i, A_i] \tag{20}$$

$$\sum_S \sum_A \varphi^{i,\pi^{-i}}(S_{i'}, A_i) = 1 \tag{21}$$

$$\varphi^{i,\pi^{-i}}(S_{i'}, A_i) \geq 0. \tag{22}$$

In this optimization problem, Eq. (18) is the objective function used to minimize the average grid energy consumption of SC i , and the constraints are expressed as Eqs. (19), (20), (21), and (22). Specifically, Eq. (19) implies that the target outage probability should always be kept lower than the desired target outage probability γ_o . The constraints in Eqs. (20), (21), and (22) respectively represent the Chapman-Kolmogorov equation and the probability properties.

The stationary best response policy of SC i can be obtained as follows:

$$\pi^{i*}(S_i, A_i) = \frac{\varphi^{i*,\pi^{-i}}(S_i, A_i)}{\sum_{A_{i'}} \varphi^{i*,\pi^{-i}}(S_i, A_{i'})}. \tag{23}$$

The constrained Nash equilibrium ensures that SC i cannot achieve a lower cost by adopting any other stationary policies while the other SCs do not change their stationary policies. To update the policies of SCs as shown in the algorithm, we apply best response dynamics [26], [27]. Note that an interaction among SCs is conducted through the probability λ^{-i} . Then, λ^{-i} can be obtained by

$$\lambda^{-i} = 1 - \prod_{i' \neq i} (1 - \lambda^{i'}), \tag{24}$$

Algorithm 1 Best Response Algorithm

- 1: Initialize the policies π^i for $\forall i$
 - 2: Share the SINR among SCs
 - 3: **repeat**
 - 4: **for** $i = 1, \dots, N$ **do**
 - 5: Calculate λ^{-i} from (23)
 - 6: Obtain π^{i*} by solving the LP problem
 - 7: **end for**
 - 8: **until** Convergence of the policies for all SCs
-

where λ^i denotes the probability that SC i conducts CoMP-JT; this can be expressed as

$$\lambda^i = \sum_{S_i \neq 0} \varphi^{i,\pi^{-i}}(S_i, A_i = 1). \tag{25}$$

G. BEST RESPONSE ALGORITHM

As shown in Algorithm 1, to begin, each SC initializes its policy (line 1 in Algorithm 1), then broadcasts its policy and CoMP-JT conduction probability to neighbor SC (line 4 in Algorithm 1). After receiving the information, each neighbor SC calculates the probability that at least one SC except SC i conducts CoMP-JT (i.e., λ^{-i}) given the policies and CoMP-JT conduction probabilities (line 5 in Algorithm 1). Then, each SC solves the LP problem to obtain the best response policy π^{i*} (line 6 in Algorithm 1).³ This procedure is repeated until the stationary policies of all SCs converge.

³In this paper, we have utilized the linprog function in Matlab 2021 to solve the LP problem. However, please note that any kinds of LP solver can be exploited.

$$P[E_{i'}|E_i, N_i, A_i = 0] = \begin{cases} \sum_{k > E_{max} - E_i} P_E(\lambda_E, k), & \text{if } E_{i'} = E_{max} \\ P_E(\lambda_E, k), & \text{if } E_{i'} = E_i + k, k \leq E_{max} - E_i \\ 0, & \text{otherwise.} \end{cases} \tag{8}$$

$$P[E_{i'}|E_i, N_i, A_i = 1] = \begin{cases} \sum_{k > E_{max} - E_i} P_E(\lambda_E, k), & \text{if } E_{i'} = E_{max} - N_i, k > E_{max} - E_i \\ P_E(\lambda_E, k), & \text{if } E_{i'} = E_i + k, k \leq E_{max} - E_i, N_i \leq E_i \\ \sum_{k < -E_i + N_i} P_E(\lambda_E, k), & \text{if } E_{i'} = 0, N_i > E_i \\ 0, & \text{otherwise.} \end{cases} \tag{9}$$

$$v(S_i, A_i) = \begin{cases} \sum_{k < -E_i + n_i} |E_i + k - N_i| P_E(\lambda_E, k) P_U(\lambda_U, k), & \text{if } A_i = 1 \\ 0, & \text{otherwise.} \end{cases} \tag{10}$$

$$c(S_i, A_i) = \begin{cases} \Pr\left[\frac{P_0 + \sum_{j=1}^n \mathcal{B}(j, \lambda^{-i})}{\sum I + \sigma^2} < \gamma_{th}\right], & \text{if } A_i = 1 \\ \Pr\left[\frac{\sum_{j=1}^n \mathcal{B}(j, \lambda^{-i})}{\sum I + \sigma^2} < \gamma_{th}\right], & \text{otherwise.} \end{cases} \tag{11}$$

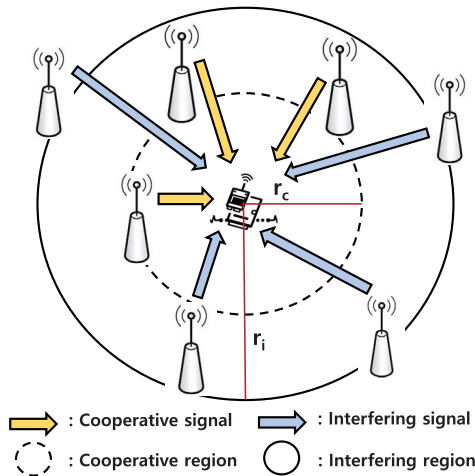


FIGURE 2. System topology.

TABLE 2. Summary parameters.

Parameter	Value
λ_E	3
λ_U	3
σ^2	-174dBm/Hz+10log ₁₀ (B_s +10dB)
B_s	1GHz
α	2
r_c	200m
r_i	300m
m	3
γ_{th}	1
γ_o	0.1
P_t	30dBm

The complexity of the proposed algorithm depends on the complexity of solving LP problem. The complexity of the Vaidya’s algorithm, that is the representative algorithm solving a LP problem, is $O((|S_i||A_i|)^3)$ [28] (i.e., polynomial time), where $|S_i|$ and $|A_i|$ denote the numbers of states and actions of SC i , respectively. Meanwhile, to reach the equilibrium, the algorithm needs only a few iterations (see Fig. 3). To sum up, the proposed algorithm can easily be implemented in real CoMP-JT systems.

V. NUMERICAL EXAMPLES

To evaluate the performance of the proposed system, we built a simulation program using MATLAB. In the downlink of mmWave cellular networks, the number of SCs that can conduct CoMP-JT is set to 4 and the interfering SCs are set to 15. To consider the outdoor dense mmWave networks, as shown in Fig. 2, the distance between user and SCs conducting CoMP-JT, $r_c = 200m$, and the distance between user and interfering SCs, $r_i = 300m$ [17], [20]. For the channel model of mmWave networks, we consider that each SC has i.i.d. Nakagami fading channel and $m = 3$ [23]. Moreover, $\alpha = 2$, $\gamma_{th} = 1$ and $P_t = 30dBm$. Table 2 lists the chosen system parameters for mmWave networks [20]. In addition, our system is compared with four schemes as follows: 1) Always, where SCs always conduct CoMP-JT; 2) P-based, where SCs conduct CoMP-JT with the probability P, where P is set to 0.8; 3) Rand, where SCs randomly conduct CoMP-JT; and 4) Non-CoMP, where SCs do not conduct CoMP-JT.

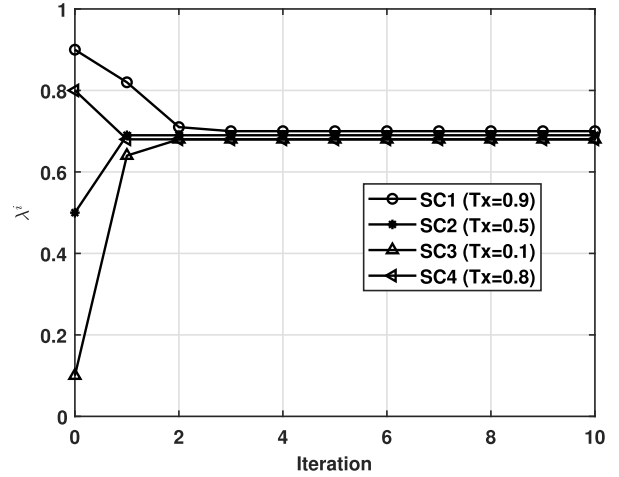


FIGURE 3. Convergence to the constrained Nash equilibrium policy, where Tx denotes the initial policy of each SC.

Fig. 3 shows the process wherein the policies of SC converge to the constrained Nash equilibrium policy. We assume that, for the initial probability to conduct CoMP-JT, SC 1 has 0.9, SC 2 has 0.5, SC 3 has 0.1, and SC 4 has 0.8. As can be seen in Fig. 3, the best response algorithm converges within a few iterations (i.e., three iterations). This means that our scheme can be implemented into the system without high overhead. We can see that each SC chooses its action by considering the other SCs actions at the best response. After the convergence, SC 1 and SC 4 with the high initial probability to conduct CoMP-JT obtain the low probability. In so doing, their grid energy consumptions can be reduced. Meanwhile, SC 2 and SC 3 with the low initial probability to conduct CoMP-JT have high probability to maintain the target outage probability.

Fig. 4 and Fig. 5 show the changes in the average grid energy consumption ψ_G and the outage probability ψ_o according to N_i , respectively, where $N_c = 3$. From these figures, we can see that our system operates adaptively in varied N_i , where, as N_i increases, the average grid energy consumption of EE-CoMP increases while keeping the target outage probability (i.e., γ_o). This is because SCs in EE-CoMP determine whether or not to conduct CoMP-JT while considering other SCs’ policies. For example, for $N_i = 8$, $\psi_G = 0.01$ and $\psi_o = 0.1$. This means that, even if a small number of SCs participate in conducting CoMP-JT, it can maintain the target outage probability. Since SCs in CoMP-JT recognize this fact, most of them do not participate in conducting CoMP-JT, which leads to diminished grid energy consumption (i.e., higher energy efficiency). On the other hand, for $N_i = 16$, to meet the target outage probability, the probability to conduct CoMP-JT of SC can be increased. Thus, the grid energy consumption is increased. On the other hand, for the other compared schemes, as N_i increases, ψ_G of these schemes increase as well. Because they do not adjust their conducting CoMP-JT policies by considering the interference level, their grid energy consumptions remain constant regardless of N_i , and their outage probabilities increase as N_i increases. We can also see that even if non-cooperation transmission scheme

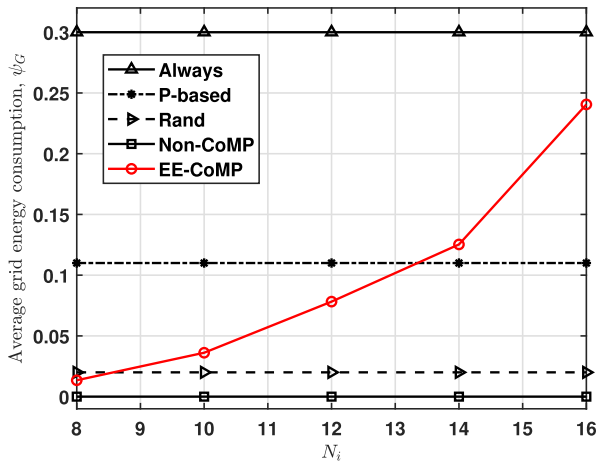


FIGURE 4. Average grid energy consumption, ψ_G versus N_i .

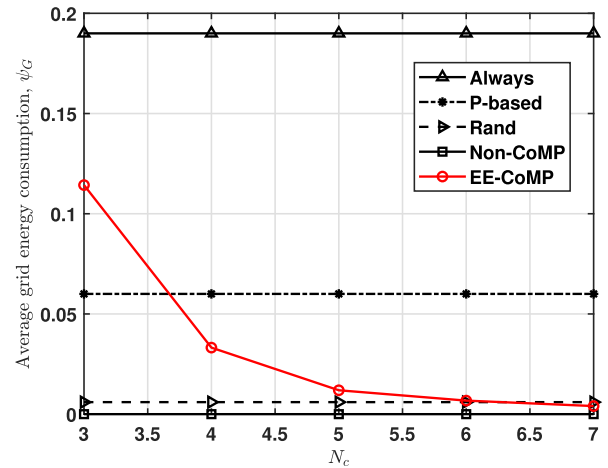


FIGURE 7. Average grid energy consumption, ψ_G versus N_c .

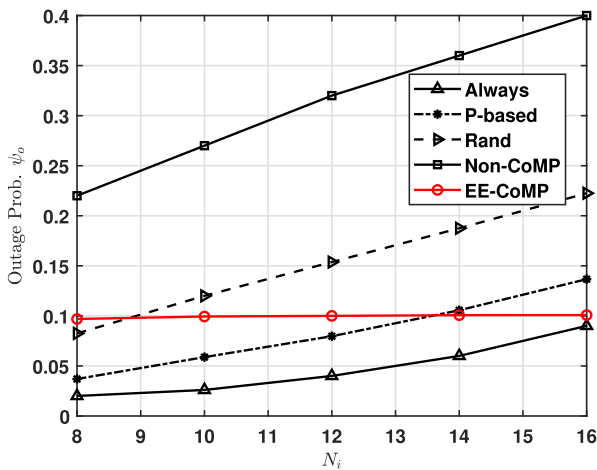


FIGURE 5. Average outage probability, ψ_o versus N_i .

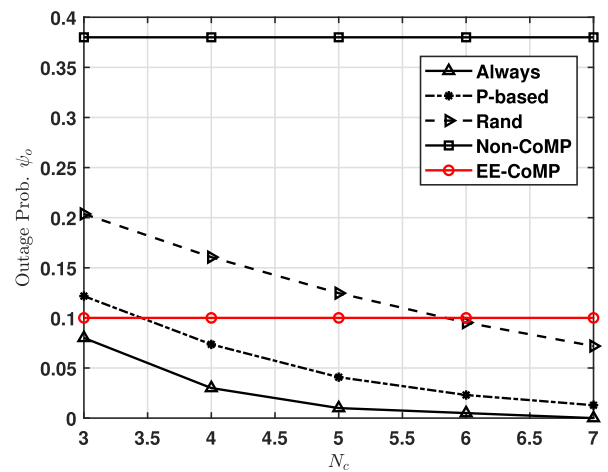


FIGURE 8. Average outage probability ψ_o versus N_c .

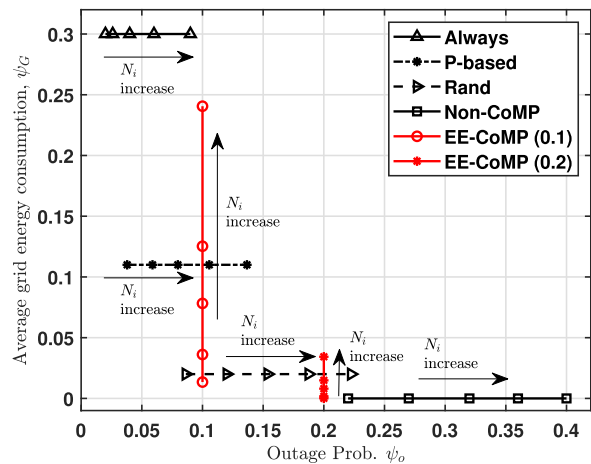


FIGURE 6. Average grid energy consumption, ψ_G versus Average outage probability, ψ_o .

(i. e., Non-CoMP) offers the low grid energy consumption, this scheme suffers from insufficient average outage probability. Specifically, CoMP-JT has an improved average outage probability when the interference power level is high.

Fig. 6 shows ψ_G with respect to ψ_o , where EE-CoMP (0.1) and EE-CoMP (0.2) respectively denote $\gamma_o = 0.1$ and 0.2.

From the vertical red line of Fig. 6, we can see that EE-CoMP can prolong ψ_G above ψ_o . That is, as N_i , ψ_G are increased and ψ_o is maintained. This is because the SCs in our system can energy-efficiently operate (i.e., SCs can reduce unnecessary conducting CoMP-JT) by considering the actions of neighbor SCs. We can also see that ψ_G cannot be decreased without increasing the tolerance of the target outage probability in the system. For example, when $\gamma_o=0.1$, ψ_G increases from 0.01 to 0.24 with increasing N_i . Meanwhile, for $\gamma_o = 0.2$, ψ_G can be maximized at 0.03.

Fig. 7 and Fig. 8 show the effect of the number of SCs that participate in the conducting CoMP-JT, i. e., N_c , on ψ_G and ψ_o , respectively, where $N_i = 15$. From these results, we can see that EE-CoMP operates adaptively when N_c is changed. That is, as N_c increases, ψ_G is decreased and ψ_o is maintained. This is because the probability to conduct CoMP-JT of SC is decreased with increasing N_c . As a result, the grid energy consumption is decreased. For example, for $N_c = 3$, $\psi_G = 0.12$. When $N_c = 7$, $\psi_G = 0.01$. We can also see that the ψ_G of other schemes remain constant regardless of N_c , because those policies are fixed. Then, the outage probabilities of other schemes decrease as N_c increases.

VI. CONCLUSION

In this paper, we propose an energy efficient CoMP-JT (EE-CoMP) scheme for the outdoor dense mmWave networks. In our scheme, SCs in the cooperative region decide whether or not to conduct a CoMP-JT by considering the actions of other SCs in a distributed manner. To minimize the grid energy consumption of SCs while maintaining the target outage probability of the system, a stochastic game model with constraints is formulated and a multipolicy is obtained by a best response algorithm. The results show that EE-CoMP can reduce the grid energy consumption by 80% compared with a probability-based scheme while providing a sufficiently target outage probability (e.g., 0.1). In our future work, to overcome the limitation (that each SC should have some statistical information) of the proposed scheme, we will introduce a multi-agent reinforcement learning approach.

REFERENCES

- [1] W. Roh, J. Y. Seol, J. Park, B. Lee, J. Lee, Y. Kim, J. Cho, K. Cheun, and F. Aryanfar, "Millimeter-wave beamforming as an enabling technology for 5G cellular communications: Theoretical feasibility and prototype results," *IEEE Commun. Mag.*, vol. 52, no. 2, pp. 106–113, Feb. 2014.
- [2] M. Giordani, M. Mezzavilla, and M. Zorzi, "Initial access in 5G mmWave cellular networks," *IEEE Commun. Mag.*, vol. 54, no. 11, pp. 40–47, Nov. 2016.
- [3] Y. Wang and Q. Zhu, "Modeling and analysis of small cells based on clustered stochastic geometry," *IEEE Commun. Lett.*, vol. 21, no. 3, pp. 576–579, Mar. 2017.
- [4] E. Turgut and M. C. Gursoy, "Coverage in heterogeneous downlink millimeter wave cellular networks," *IEEE Trans. Commun.*, vol. 65, no. 10, pp. 4463–4477, Oct. 2017.
- [5] J. Zhao, S. Ni, L. Yang, Z. Zhang, Y. Gong, and X. Yu, "Multiband cooperation for 5G HetNets: A promising network paradigm," *IEEE Veh. Technol. Mag.*, vol. 14, no. 4, pp. 85–93, Dec. 2019.
- [6] L. Cheng, M. M. U. Gul, F. Lu, M. Zhu, J. Wang, M. Xu, X. Ma, and G.-K. Chang, "Coordinated multipoint transmissions in millimeter-wave radio-over-fiber systems," *J. Lightw. Technol.*, vol. 34, no. 2, pp. 653–660, Jan. 15, 2016.
- [7] G. R. MacCartney and T. S. Rappaport, "Millimeter-wave base station diversity for 5G coordinated multipoint (CoMP) applications," *IEEE Trans. Wireless Commun.*, vol. 18, no. 7, pp. 3395–3410, Jul. 2019.
- [8] S.-Y. Kim and C.-H. Cho, "Call blocking probability and effective throughput for call admission control of CoMP joint transmission," *IEEE Trans. Veh. Technol.*, vol. 66, no. 1, pp. 622–634, Jan. 2017.
- [9] M. Gapeyenko, V. Petrov, D. Moltchanov, M. R. Akdeniz, S. Andreev, N. Himayat, and Y. Koucheryavy, "On the degree of multi-connectivity in 5G millimeter-wave cellular urban deployments," *IEEE Trans. Veh. Technol.*, vol. 68, no. 2, pp. 1973–1978, Feb. 2019.
- [10] L. Chettri and R. Bera, "A comprehensive survey on Internet of Things (IoT) toward 5G wireless systems," *IEEE Internet Things J.*, vol. 7, no. 1, pp. 16–32, Jan. 2020.
- [11] Y.-K. Chia, S. Sun, and R. Zhang, "Energy cooperation in cellular networks with renewable powered base stations," *IEEE Trans. Wireless Commun.*, vol. 13, no. 12, pp. 6996–7010, Dec. 2014.
- [12] A. Balakrishnan, S. De, and L.-C. Wang, "Network operator revenue maximization in dual powered green cellular networks," *IEEE Trans. Green Commun. Netw.*, vol. 5, no. 4, pp. 1791–1805, Dec. 2021.
- [13] H. A. H. Hassan, D. Renga, M. Meo, and L. Nuaymi, "A novel energy model for renewable energy-enabled cellular networks providing ancillary services to the smart grid," *IEEE Trans. Green Commun. Netw.*, vol. 3, no. 2, pp. 381–396, Jun. 2019.
- [14] A. Balakrishnan, S. De, and L.-C. Wang, "Energy sharing based cooperative dual-powered green cellular networks," in *Proc. IEEE Global Commun. Conf. (GLOBECOM)*, Madrid, Spain, Dec. 2021, pp. 1–6.
- [15] B. Li, Y. Dai, Z. Dong, E. Panayirci, H. Jiang, and H. Jiang, "Energy-efficient resources allocation with millimeter-wave massive MIMO in ultra dense HetNets by SWIPT and CoMP," *IEEE Trans. Wireless Commun.*, vol. 20, no. 7, pp. 4435–4451, Jul. 2021.
- [16] L. Liu, Z. Zhang, N. Wang, H. Zhang, and Y. Zhang, "Online resource management of heterogeneous cellular networks powered by grid-connected smart micro grids," *IEEE Trans. Wireless Commun.*, early access, Apr. 15, 2022, doi: 10.1109/TWC.2022.3165975.
- [17] C. García Ruiz, A. Pascual-Iserte, and O. Muñoz, "Analysis of blocking in mmWave cellular systems: Application to relay positioning," *IEEE Trans. Commun.*, vol. 69, no. 2, pp. 1329–1342, Feb. 2021.
- [18] M. Gerasimenko, D. Moltchanov, M. Gapeyenko, S. Andreev, and Y. Koucheryavy, "Capacity of multicconnectivity mmWave systems with dynamic blockage and directional antennas," *IEEE Trans. Veh. Technol.*, vol. 68, no. 4, pp. 3534–3549, Apr. 2019.
- [19] D. Kumar, S. Joshii, and A. Tölöli, "Latency-constrained highly reliable mmWave communication via multi-point connectivity," *IEEE Access*, vol. 10, pp. 32822–32835, 2022.
- [20] L. Yang, M. Xia, and M. Motani, "Unified analysis of coordinated multipoint transmissions in mmWave cellular networks," *IEEE Internet Things J.*, vol. 9, no. 14, pp. 1–10, Dec. 2021.
- [21] M. A. Arfaoui, A. Ghayeb, C. Assi, and M. Qaraqe, "CoMP-assisted NOMA and cooperative NOMA in indoor VLC cellular systems," *IEEE Trans. Commun.*, vol. 70, no. 9, pp. 6020–6034, Sep. 2022.
- [22] S. Euttamarajah, Y. H. Ng, and C. K. Tan, "Energy-efficient joint power allocation and energy cooperation for hybrid-powered comp-enabled HetNet," *IEEE Access*, vol. 8, pp. 29169–29175, 2020.
- [23] J. G. Andrews, T. Bai, M. N. Kulkarni, A. Alkhateeb, A. K. Gupta, and R. W. Heath, Jr., "Modeling and analyzing millimeter wave cellular systems," *IEEE Trans. Commun.*, vol. 65, no. 1, pp. 403–430, Jan. 2017.
- [24] E. Altman, K. Avrachenkov, N. Bonneau, M. Debbah, R. El-Azouzi, and D. S. Menasche, "Constrained cost-coupled stochastic games with independent state processes," *Oper. Res. Lett.*, vol. 36, no. 2, pp. 160–164, Mar. 2008.
- [25] Y. Kim, M. Paik, B. Kim, H. Ko, and S.-Y. Kim, "Neighbor-aware non-orthogonal multiple access scheme for energy harvesting Internet of Things," *Sensors*, vol. 22, no. 2, p. 448, Jan. 2022.
- [26] S.-Y. Kim and Y.-K. Kim, "An energy efficient UAV-based edge computing system with reliability guarantee for mobile ground nodes," *Sensors*, vol. 21, no. 24, p. 8264, Dec. 2021.
- [27] U. Berger, "Best response dynamics for role games," *Int. J. Game Theory*, vol. 30, no. 4, pp. 527–538, May 2002.
- [28] R. J. Vanderbei, *Linear Programming: Foundations and Extensions*. New York, NY, USA: Springer-Verlag, 1997.
- [29] X. Wang, J. Gong, C. Hu, S. Zhou, and Z. Niu, "Optimal power allocation on discrete energy harvesting model," *EURASIP J. Wireless Commun. Netw.*, vol. 2015, no. 1, pp. 1–14, Dec. 2015.



SEUNG-YEON KIM received the Ph.D. degree in electronics and information engineering from Korea University, Sejong, South Korea, in 2012. He is currently an Assistant Professor with the Department of Computer Convergence Software, Korea University. His research interests include 6G networks, network automation, mobile cloud computing, federated learning, and the Internet of Things.



HANEUL KO (Member, IEEE) received the B.S. and Ph.D. degrees from the School of Electrical Engineering, Korea University, Seoul, South Korea, in 2011 and 2016, respectively. From 2016 to 2017, he was a Postdoctoral Fellow in mobile network and communications, Korea University, Seoul. From 2017 to 2018, he was a Postdoctoral Fellow at the University of British Columbia, Vancouver, BC, Canada. From 2019 to 2022, he was an Assistant Professor at the Department of Computer and Information Science, Korea University, Sejong, South Korea. He is currently an Assistant Professor with the Department of Electronic Engineering, Kyung Hee University, Yongin, South Korea. His research interests include 5G/6G networks, network automation, mobile cloud computing, SDN/NFV, and the future internet.

• • •